Proteins and signaling pathways response to Wenjingtongluo drug-contained serum in IHUVECs: an explorative proteomic study

Weimin Xu[1#], Jiajia Qian[1#, 3*], Qi Xu[2#], Ren Cai[4], Guo Yang[1], Jiarong Wei[5], Guicheng Huang[1*]

[1] Laboratory for New Techniques of Restoration & Reconstruction of Orthopedics and Traumatology, Nanjing University of Chinese Medicine, Nanjing, 210023, Jiangsu, China

[2] Graduate School of Anhui University of Chinese Medicine, HeFei, 230000, Anhui, China

[3] Department of Rehabilitation Therapy, Nanjing University of Chinese Medicine, Nanjing, 210023, Jiangsu, China

[4] Department of Basic Physical Education, Nanjing University of Chinese Medicine, Nanjing, 2100223, Jiangsu, China

[5] HeJinTang Traditional Chinese Medicine Clinic, Nanjing, 210003, Jiangsu, China

#This author contributes equally to this paper.

ARTICLE INFO

ABSTRACT

Angiogenesis is a dynamic and complex process leading to the development of new vessels from pre-existing vessels, which played a major role in pathological processes in many diseases. The present study aimed to investigate the effect of drug-contained serum of Traditional Chinese medicine (TCM) Wenjingtongluo decoction (WJLTD) on antiangiogenesis in Immortalized Human Umbilical Vascular Endothelial cells (IHUVECs), and elucidate the possible mechanisms based on proteomic analysis. Cells were treated with the drug-contained serum of the Drug-contained Serum (DS) of WJLTD and the blank serum (BS). The antiangiogenesis capacity of DS was evaluated using wound healing assay, Transwell, and tube formation assay. We performed three biological replicates to compare large-scale differential protein expression between two groups by tandem mass tag (TMT) labeling technology based on liquid chromatography-mass spectrometry analysis (LC-MS/MS). Gene Ontology (GO), Kyoto Encyclopedia of Genes and Genomes (KEGG) enrichment analyses were performed for the general characterization of overall enriched proteins. For validation of the results of TMT, the candidate proteins were verified by parallel reaction monitoring (PRM) analysis. The results showed that 4% DS could inhibit the migration process of IHUVECs according to wound healing assay and Transwell. And tube formation ability was also dramatically inhibited (p<0.001). TMT analysis revealed 148 differentially expressed proteins between two groups that were identified and quantified. The further validation results of the two candidate proteins, Ferritin heavy chain (FTH1) and Ferritin light chain (FTL) from the Ferroptosis pathway, which played an important role in DS treatment, were consistent with those of LC-MS/MS. In conclusion, this is the first proteomics-based study to report the mechanism underlying DS treatment for angiogenesis. Further functional verification of the potential signaling pathways and the enriched proteins is warranted.

Introduction

Angiogenesis is a dynamic and complex process leading to the development of new vessels from pre-existing vessels (1,2). Angiogenesis is essential for growth and development, the reproductive cycle, and tissue repair which occurs under physiological conditions during normal wound healing (3). In addition, angiogenesis plays a major role in pathological conditions such as diabetic retinopathy, rheumatoid arthritis, osteoarthritis, cardiovascular diseases and tumor (4-7). So the antiangiogenic molecules, such as Bevacizumab, an anti-vascular endothelial growth factor (VEGF) antibody, are often used in the treatment of many diseases according to recent guidelines (8,9). Traditional Chinese medicine has been proven to play a significant role in antiangiogenesis.

Wenjingtongluo decoction (WJLTD), a Traditional Chinese medicine prescription, is a clinical experience formula of Prof. Guicheng Huang based on the theory of the Wenjingtongluo method for the treatment of the cold-dampness syndrome. Studies have shown that the Wenjingtongluo method can intervene in angiogenesis and participate in the regulation of rheumatoid arthritis by regulating the VEGF-related signal pathway and its receptor (10,11). Our previous studies also confirmed that Wenjingtongluo Decoction can inhibit HIF-1α/VEGF and VEGF /VEGFR2/ERK1/2 signaling pathway, regulate angiogenesis in cartilage and delay the pathological process of osteoarthritis (12,13). Nevertheless, the molecular mechanism of WJLTD in regulating angiogenesis remains unclear. HUVECs were often applied for investigating endothelial physiology and angiogenesis. Here, for the first time, we used HUVECs as cell models to explore the mechanisms of WJTLD in antiangiogenesis.

Traditional Chinese medicine (TCM) compound can play an integrated role from multi-level, multi-link and

multi-target. Therefore, we speculated that WJLTD also can inhibit angiogenesis through multiple levels of gene regulation. Proteomics has been used in the study of TCM for many years, researches mainly focus on the exploration of possible therapeutic targets (14,15). Tandem mass tag (TMT) is one of the relative quantitative proteomics technologies, which can simultaneously label and analyze multiple biological samples, and further outputs precise sensitivity and high-quality data (16). Recently, TMT combined with LC-MS/MS analysis has become a powerful tool in the identification, characterization, and quantitation analysis of proteomic profiles (17,18). Which overcomes the deficiencies of traditional methods when macromolecules and proteins cannot be quantified (19).

In this study, we investigated the effect of WJTLD on inhibiting angiogenesis and applied TMT quantitative proteomics technology to detect differentially expressed proteins in the Immortalized Human Umbilical Vascular Endothelial cells (IHUVECs), and to elucidate the possible mechanisms of WJTLD based on bioinformatics analysis. Furthermore, major proteins were verified by parallel reaction monitoring (PRM) analysis. This work demonstrates the possible mechanisms of WJTLD in antiangiogenic and provides proteomics evidence for treatment with WJTLD.

Materials and Methods

Drug-contained serum preparation

WJLTD used in the present study was provided by Jiangsu Province Hospital of TCM (China), which includes: 10g Fuzi (Aconiti Lateralis Radix Praeparata), 8g Guizhi (Cinnamomi Ramulus), 10g Zexie (Alismatis Rhizoma), 25g Tufuling (Smilacis Glabrae Rhizoma),10g Chenpi (Citri Reticulatae Pericarpium),15gYanhusuo (Corydalis Rhizoma), 2g Wugong (Scolopendra), 3g Quanxie (Scorpio), 6g Dannanxing (Arisaema Cum Bile), 25g Shudihuang (Rehmanniae Radix Praeparata), 10g Niuxi (Achyranthis Bidentatae Radix) and 10g Gancao (Glycyrrhizae Radix et Rhizoma). After being immersed in 1072 mL distilled water for 30 min, Fuzi was decocted first for 30 min, then boiled for 45 min with other components, then decocted in 1072 distilled water again. After each decoction, the gauze was used for filtration and the liquid was merged and concentrated into a liquid that contained 1.4g/ml.

Ten Sprague Dawley (SD) male rats (200±20g) were purchased from the Animal Center of Qinglongshan (Nanjing, China). Rats were randomly divided into two groups: the Drug-contained Serum (DS) group and the Blank Serum (BS) group, with 5 rats in each group. WJLTD was respectively given to rats(1ml/100g/day) by gastrogavage for 7 successive days, normal saline in the same volume was given to rats in the normal control group by gastrogavage. The blood was withdrawn from the Abdominal aorta 1.5 h after the last gastrogavage. The serum was isolated after centrifuge (3000r/min) for 15 min. After filtration with the 0.22μm microporous membrane and inactivation at 56°C for 30 min, the serum was kept at -80°C. This study was approved by the Ethics Committee of the Nanjing University of Chinese Medicine.

Cell culture

Immortalized Human Umbilical Vein Endothelial Cells (IHUVECs-SV40) obtained from Abmgood, China, and cultured in TM001 medium, supplementation with 10% fetal bovine serum, and 1% penicillin and streptomycin (P/S) at 37°C in a humidified cell culture supplied with 5% CO_2.

CCK-8 assay of cell proliferative inhibition rate

Cell proliferative inhibition rate was measured by cell counting kit-8 (CCK-8, Vazyme, A311, China). IHUVECs were seeded in 96-well plates at a density of 1×10^5 cells/mL and then treated with different concentrations of DS and BS (0,2,4,8,12%), for 0,24,48 and 72h. After washing three times with PBS, cells were incubated with CCK-8 solution and TM001media (1:10 dilution) at 37°C for 1h, then measured absorbance at 450nm by a microplate reader.

Wound healing assay

IHUVECs were planted in 6-well plates. When IHUVECs monolayer cultures reached approximately 80% confluency, three scratches were made using a 200-μl pipette tip across the plates. After plates were washed with PBS,2mL TM001 medium was added, IHUVECs were grown for 0h and 48h and photographs were taken at different time points.

Transwell assay

The upper side of the basement membrane of the Transwell chambers was coated by using a Matrigel dilution (1:8) and dried at room temperature. After a conventional detachment process, the cells were washed using PBS two times followed by resuspension in TM001 medium with the cell density having been adjusted to 1×10^5 cells/mL. Then, 200μl cell suspension was added into the Matrigel-coated apical chambers, while the basolateral chambers were added with 600μl TM001 medium. After a conventional culture for 24h, the Transwell chambers were subsequently taken out, and washed with PBS three times. The sample was then fixed for 10 min, and stained using crystal violet for 15min. Five visual fields were selected on a random basis under an inverted microscope (100×, Olympus, IX51, Japan) with pictures taken. The number of cells that migrated through the membrane was counted. Three replicate wells were set for each group and the average value was calculated.

Tube formation assay

The in vitro angiogenesis capacity of IHUVECs was evaluated using the tube formation assay (20), 100 mL Matrigel (BD,354234, USA) was added into each well of a 96-well plate, which was kept in a cell culture chamber for 30 min to facilitate solidification. IHUVECs were collected, and cell suspension densities were adjusted to 1×10^4 cells/mL. Approximately 60 mL cell suspension was added into each well, followed by culture in a cell chamber and observation of tube formation. For comparison, three biological replicates were performed.

Tandem Mass Tag (TMT) labeled quantitative proteomics

Experimental procedures

Sample Preparation

SDT buffer was added to IHUVECs. The lysate was

sonicated and then boiled for 15 min. After centrifuging at 14000g for 40 min, the supernatant was quantified with the BCA Protein Assay Kit (P0012, Beyotime). The sample was stored at -20°C.

SDS-PAGE Separation

20μg proteins were added with 6X loading buffer for each sample and boiled for 5min. Then the proteins were separated on 12% SDS-PAGE gel. Protein bands were visualized by Coomassie Blue R-250 staining.

Filter-aided sample preparation (FASP Digestion)

200μg proteins of each sample were incorporated into 30μl SDT buffer. The detergent, DTT and other low-molecular-weight components were removed using UA buffer through repeated ultrafiltration (Sartorius, 30kD).100μl iodoacetamide was added in order to block reduced cysteine residues, then samples were incubated for 30min in darkness, and centrifuged at 12500×g for 25 min. The filters were washed with 100μl UA buffer three times and then 100μl 0.1M TEAB buffer twice. At last, the samples were digested with 40μl trypsin buffer overnight at 37°C, then collecting the filtrate. The peptide content was estimated by UV light spectral density at 280nm.

TMT Labeling

100μg peptide mixture of each sample was labeled using TMT reagent according to the manufacturer's instructions (Thermo Fisher Scientific, USA).

Peptide Fractionation with reversed phase (RP) Chromatography

TMT-labeled peptides were fractionated with RP chromatography using the Agilent 1260 infinity II HPLC. The peptide mixture was diluted with buffer A (10mM HCOONH4, 5%ACN, pH 10.0) and loaded onto an XBridge Peptide BEH C18 Column. Then peptides were eluted at a flow rate of 1 ml/min with a gradient of 0%-7% buffer B (10mM HCOONH4,5% ACN, pH 10.0) for 5 min,7-40% buffer B in 5 to 40min,40%-100% buffer B in 45 to 50 min,100% buffer B in 50 to 65min. The elution was monitored at 214 nm, and fractions were collected every 1 min for 5 to 50min. The fractions were combined into 10 fractions and dried at 45°C.

Mass Spectrometry analysis

Easy nLC chromatography

Each fraction was injected for nanoLC-MS/MS analysis. The peptide mixture was loaded onto the C18-reversed phase analytical column (Thermo Fisher Scientific, Acclaim PepMap RSLC 50um X 15cm, nano viper, P/N164943) in buffer A (0.1% Formic acid) and separated with a linear gradient of buffer B (80% acetonitrile and 0.1% Formic acid) at a flow rate of 300 nl/min. The linear gradient used 1.5 hours gradient: 6% buffer B for 5 min, 6-28% buffer B for 63 min,28-38% buffer B for 10 min,38-100% buffer B for 7 min, hold in 100% buffer B for 5 min.

LC-MS/MS Analysis

LC-MS/MS analysis was performed on a Q Exactive mass spectrometer (Thermo Fisher Scientific) that was coupled to Easy nLC (Thermo Fisher Scientific) for 90min. The mass spectrometer was operated in positive ion mode. MS data were acquired using a data-dependent top10 method dynamically choosing the most abundant precursor ions from the survey scan (350-1800m/z) for HCD fragmentation. Survey scans were acquired at a resolution of 70000 at m/z 200 with an AGC target of 3e6 and a maxIT of 50 ms. MS2 scans were acquired at a resolution of 17500 for HCD spectra at m/z 200 with an AGC target of 2e5 and a maxIT of 45ms, and the isolation width was 2m/z. Only ions with a charge state between 2-6 and a minimum intensity of 2e3 were selected for fragmentation. Dynamic exclusion for selected ions was the 30s. The normalized collision energy was 30eV.

Bioinformatics Analysis

A bioinformatics analysis between the two groups was performed. Firstly, all protein sequences were aligned to the Linux database downloaded from NCBI, only the sequences in the top 10 and E-value<=1e-3 were kept. Then the Gene Ontology (GO) term of the sequence with the top Bit-Score by Blast2GO was selected. Next, the annotation from GO terms to proteins was completed by Blast2GO Command Line (www.geneontology.org). After the elementary annotation, InterProScan was used to search the EBI database by motif, then add the functional information of motif to proteins to improve annotation. Then further improvement of annotation and connection between GO terms were carried out by ANNEX. Using Fisher's Exact Test to enrich GO terms by comparing the number of differentially expressed proteins and total proteins correlated to GO terms. Pathway analysis was performed using the Kyoto Encyclopedia of Genes and Genomes (KEGG) database. Fisher's Exact Test was used to identify the significantly enriched pathways by comparing the number of differentially expressed proteins and total proteins correlated to pathways.

We employed the WoLF PSORT (https://wolfpsort.hgc.jp/) to predict the localization of differential proteins and used the InterPro database to perform functional domain annotation analysis. Matplotlib software was used to classify the expression of samples and proteins in two dimensions simultaneously and generate a hierarchical clustering heat.

IPA analysis

The proteins affected by WJTLD DS on IHUVECs were analyzed by Ingenuity Pathways Analysis (IPA) network.

Parallel Reaction Monitoring (PRM) Validation

To verify the results of TMT analysis coupled with liquid chromatography-mass spectrometry analysis (LC-MS/MS), PRM was performed among all proteins of differential abundance under each condition. Two proteins of interest, namely, ferritin heavy chain (FTH1) and ferritin light chain (FTL) were selected for analysis.

1μg sample of each group was injected and separated by nano-LC and analyzed by online electrospray tandem mass spectrometry. The complete liquid-mass tandem system was 1) Liquid phase system: Easy nLC system (Thermo Fisher Scientific) 2) Mass spectrometry system: Q-Exactive HFX (Thermo Fisher Scientific). Buffer A solution was 0.1% formic acid aqueous solution, and buffer B solution was 0.1% formic acid acetonitrile aqueous solution (80% acetonitrile). Samples were separated at a flow

rate of 300 nL/min through the analytical column (Thermo Fisher Scientific, Acclaim PepMap RSLC 50um X 15cm, nano viper, P/N164943) with a non-linearly increasing gradient: from 0min to 5min, liquid B 1 to 3%; from 6min to 45min, B liquid linear gradient from 3%-28%; from 46min to 50min, B liquid linear gradient from 28%-38%; 51min to 55min, B liquid linear gradient from 38%-100%; 56min to 60min, B liquid maintained at 100%. The mass spectrometry parameters were set as follows: (I) full MS: scan range (M / z) = 350-1800; resolution=60,000; AGC target=3e6; maximum injection time=50ms; (II) PRM: resolution=30,000; AGC target=2e5; maximum injection time=50ms; Loop count=10; Isolation window=2.0m/z; NCE=27eV.

Statistical Analysis

Proteins with Fold change>1.2 and p-value (Student's T test) <0.05 were considered to be differentially expressed proteins. Statistical analysis was performed with Graph-Pad Prism 8, results were compared by one-way analysis of variance (ANOVA). All data were expressed as mean ± standard deviation(SD), and a P-value<0.05 was considered statistically significant.

Results

Effect of DS on cell proliferative inhibition rate

CKK-8 assay showed that the inhibition rate of 4%DS for 48h was significant (*P*<0.05). According to the result, the following experiment selected 4%DS intervention for 48h as the experimental condition (Figure 1).

Effect of DS on inhibiting the migration of IHUVECs

Cell migration is one of the hallmarks of angiogenesis and occurs in the earlier steps of the angiogenic cascade (21). Wound healing and Transwell test were detected to access the capacity of DS on inhibiting the migration of IHUVECs. A wound healing assay was performed to investigate the inhibition effect of 4% DS for 48h. As Figure 2A and Figure 2B shown, treatment with 4% DS declined the wound closure rate. In Figure 2C and Figure 2D, the results showed that, compared with the BS group, the number of cell migrations in 4% DS group decreased significantly. Taken together,4% DS could inhibit the migration process of IHUVECs.

Effect of DS on inhibiting the tube formation of IHUVECs

A tube formation assay was carried out to test the effect of DS on the formation of chord-like networks in HU-

VECs. The capillary-like tubes were observed after 48h of incubation with BS and DS. As shown in Figure 3, 4% DS dramatically inhibited capillary tube formation. Therefore, DS could inhibit IHUVECs network formation.

TMT analysis of differentially expressed proteins

A total of 61926 peptides and 6921 proteins were identified in this experiment, and 148 differentially expressed proteins between groups were identified and quantified (Supplementary Materials). Of these, 87 proteins were Up-regulated and 61 proteins were down-regulated. These
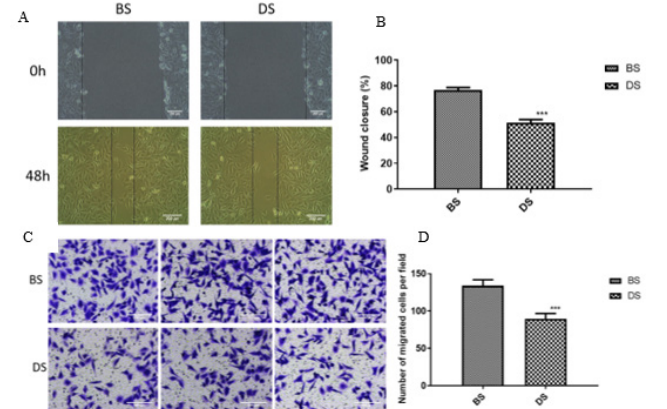

Figure 2. DS inhibited the migration of IHUVECs. A. IHUVECs were scratched by pipette tips to produce the wound (shown between the two black lines in each photo) and then were treated with 4%WJTLD DS and BS for 48h. Then photographed under inverted microscope, Scale bar=200μm. B. Wound closure rate of IHUVECs. C. IHUVECs invasion detected by Transwell assay, Scale bar=100μm. D. Number of migrated cells in each group was quantified by Image-J. *p<0.05; **p<0.01; ***p<0.001. The data were analyzed by one-way ANOVA followed by Dunnett's test for comparisons of two groups.

Figure 3. IHUVECs angiogenesis detected by tube formation assay. Scale bar=200μm. IHUVECs were treated with DS and BS for 48 h. The tubes were photoed under an inverted microscope. The Capillary-like structure number in each group was quantified by Image-J. *p<0.05; **p<0.01; ***p<0.001. The data were analyzed by one-way ANOVA followed by Dunnett's test for comparisons of all treated groups with the control group.

Figure 1. IHUVECs were plated in 96-well culture plates. After 24h, different concentrations of BS and DS (0%, 2%, 4%, 8%, 12%, 16) were added. After 0h, 24 h, 48h, and 72h of treatment, cell viability was measured by CCK-8 assay.

Figure 4. Volcano plot of significantly differentially expressed proteins of two groups.

proteins will be used for further analysis.

The results of significant differences between the two groups were presented by plotting volcano plots. Blue dots (left) represent the number of downregulated proteins and red dots (right) represent the number of upregulated proteins. Specific results are presented in Figure 4.

Bioinformatics analysis

GO analysis

To further investigate the regulatory mechanism of DS on IHUVECs, GO function annotation and pathway enrichment analysis were performed on the differential expression of proteins from three aspects: biological process (BP), molecular function (MF) and cellular component (CC).

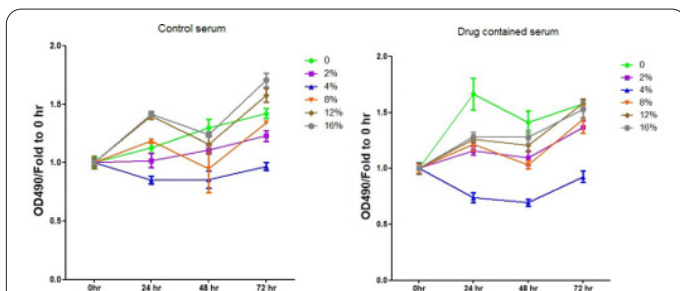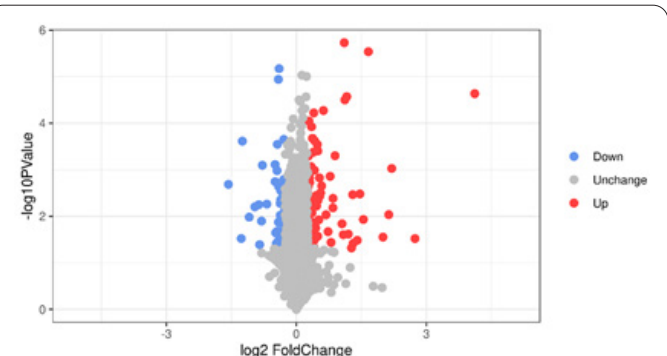The results of BP-related pathway analysis show that these differential proteins were mainly involved in the following aspects:①positive regulation of chondrocyte proliferation, and the related differential proteins are TF, LTF;②negative regulation of blood platelet activation, related differential proteins are ANGPTL4, APOE;③acute inflammatory response to antigenic stimulus, related differential proteins include SERPINC1;④bone morphogenesis, related differential proteins include HPX, VTN, etc.;⑤positive regulation of TRAIL-activated apoptotic signaling pathway, and the related differential proteins are TIMP3 and FOSL2.

MF analysis revealed that the main functions of differentially expressed proteins include: ① positive regulation of blood vessel endothelial cell migration: the relevant differential proteins include VEGFR2 and ANGPTL4; ②negative regulation of blood vessel endothelial cell migration: the relevant differential proteins include APOE, etc.; ③positive regulation of angiogenesis: associated differential proteins have VEGFR2, etc.; ④negative regulation of the apoptotic process, in which the differential proteins include VEGF-A, PIK3R, etc.; ⑤extracellular matrix binding, among which the differential proteins include VEGF-A, TGFBI, VTN, etc. Among these, VEGF-A and VEGFR2 pathway has been proven to be involved in regulating angiogenesis in the pathological process of OA (22).

The results of CC analysis indicate that: ① mitochondrial intermembrane protein transporter complex, related differential proteins are TIMM8A, TIMM13, etc.; ②intracellular ferroportin complex, and the related differential proteins were FTL, FTH1.

Figure 5 showed the top 10 pathways with high enrichment analyzing from the above three aspects.

KEGG pathway enrichment analysis

The method of KEGG pathway enrichment analysis is similar to the GO enrichment analysis in that it is based on all qualitative proteins in terms of the KEGG pathway by Fisher's exact test, and the significance level of protein enrichment for each pathway is analyzed as a way to identify signal transduction pathways that exert a significant influence. The results of the pathway analysis demonstrated that there were 10 pathways with significant differences (p<0.05) in the higher enrichment after the intervention of WJTLT-containing serum and blank serum, including Ferroptosis, the relevant differential proteins are FIH1, FTL; Complement and coagulation cascades; Mineral absorption; Cholesterol metabolism; Staphylococcus aureus infection; Systemic lupus erythematosus; PPAR signaling pathway; Neuroactive ligand-receptor interaction; Sesquiterpenoid and triterpenoid biosynthesis; Cutin, suberine and wax biosynthesis. Figure 6 displays the top 10 signal pathways with higher enrichment.

Subcellular localization analysis

Software WoLF PSORT was used to locate 149 differential proteins. The results showed that differential proteins were distributed outside the cell, cytoplasm, nucleus and cell membrane, indicating that the proteins affected by the DS did not show a preference for subcellular localization. The specific results are shown in Figure 7.

Figure 6. Statistical bubble plot of significantly enriched KEGG pathways (top 10).

Figure 5. Columnar statistics of GO annotation results (top 10).

Figure 7. Protein subcellular localization profiles.

Domain annotation and enrichment analysis

Domains are the basic units of protein structure, function and evolution (23). In this research, the annotation and enrichment of the functional domains of different proteins are analyzed using the Interpro database, and the first ten protein domains with the highest concentrations are screened. The specific results are shown in Figure 8.

Cluster analysis

Clustering results showed that after the treatment of DS, the changes in the expression of different proteins formed a significant distinction between the two groups, and showed good consistency under three biological repetitions in each group. Indicating that changes in target differential protein expression can represent a significant effect of DS treatment. The specific results are shown in Figure 9.

PRM Validation of TMT and IPA-Based Results

To explore the molecular mechanism of WJTLD in regulating angiogenesis deeply, and considering the relevant research hotspots, we further applied IPA software to analyze the function of differential proteins. According to the TMT mass spectrometry identification and IPA analysis, two proteins of interest were selected for PRM validation, including FTH1, and FTL. After normalization, the results of the relative quantitative expression revealed in Figure 10, the fold change of 2 candidate proteins were found to be significant according to both TMT and PRM analysis.

Discussion

Angiogenesis is a pivotal process in embryo development, tissue growth and wound healing (24). Pathologically, angiogenesis can promote inflammation, abnormal wound healing, vascular diseases, and tumor development and progression (25). Thus, angiogenesis may be a therapeutic target for various diseases (26). HUVECs are derived from the vascular endothelium of the umbilical cord. Because of their low cost and relatively easy operation and collection, they have been applied as cell models for investigating endothelial physiology and angiogenesis (27). However, primary HUVECs have a very limited ability to proliferate in vitro. Since they enter a growth stagnation period known as replicative senescence after a certain number of cell divisions (28). And senescent cells experience both morphological changes and functional losses (29), which makes primary HUVECs difficult to apply on a large scale. Now, immortalized cell lines have been established successfully by transduction of simian vacuolating virus 40 large T antigen (30) or telomerase reverse transcriptase (TERT) (31), such as IHUVECs. These cells are easy to handle, stable, and have been used in many studies.

During angiogenesis, endothelial cells migrate, proliferate and organize into tubular structures, which play an active role in tissue remodeling (32). Here, we investigated the effects of drug-contained serum of WJLTD and blank serum on IHUVECs proliferation, migration and tube formation in vitro, so as to explore the inhibitory effect of WJLTD on angiogenesis. In vitro experiments, we showed that after 4%DS treatment, the migration and capillary tube formation of IHUVECs were significantly inhibited, demonstrating superior anti-angiogenic activity. However, the potential mechanisms remain unknown.
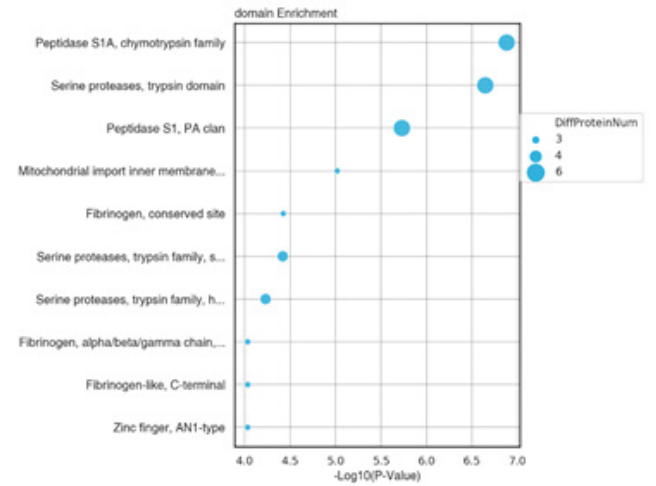

Figure 8. Bubble plot of significantly enriched protein domain classifications statistics.
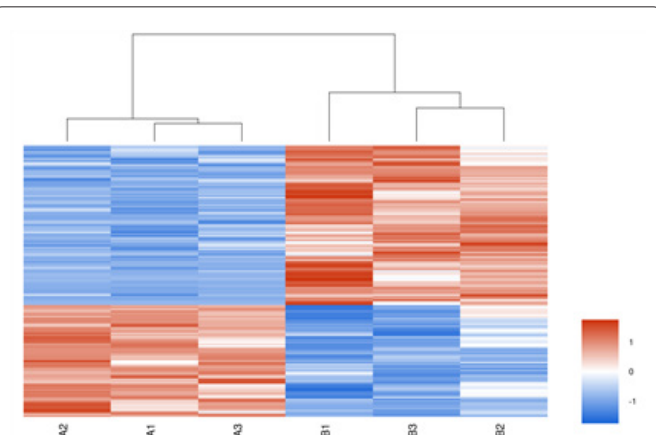

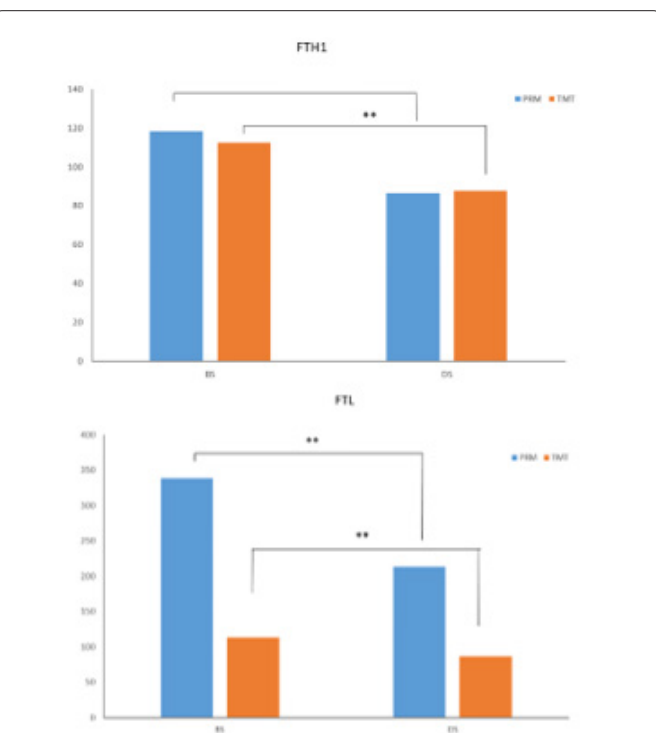**Figure 9.** Cluster analysis results.

Figure 10. PRM and TMT protein expression quantities of the two candidate proteins. Abbreviations: TMT, tandem mass tag; PRM, parallel reaction monitoring. Data are shown as mean ± SD: ** $p<0.01$, compared to BS. The proteins relative amount in PRM×10^4.

In our study, three biological replicates were performed to compare the large-scale differential protein expression between two groups by TMT labeling relative to quantitative proteomics technology. In the present work,148 significantly differential proteins were identified in two groups. PRM is an emerging technique based on high-resolution MS platforms, used for the quantification of target proteins in complex biological samples (33). PRM collects all the fragment ions after the fragmentation of the precursor ion, resulting in better reliability and specificity (34). The PRM method is conceptually similar to Western Blotting(WB), but is independent of the specificity of the antibody, making it superior to WB, especially when a high-quality antibody is unavailable (35). Additionally, we verified two differentially expressed candidate proteins using MS-based precise quantitative PRM analysis, and the results showed similar trends as those observed in TMT analysis. Hence, the results of these experiments are technically reliable.

GO and KEGG enrichment results indicated that DS treatment significantly regulated the Ferroptosis pathway. Ferroptosis, a new type of programmed cell death, was first observed in cancer cells with oncogenic Ras mutations, which are characterized by excessive iron-dependent lipid peroxidation (36,37). Previous studies highlight the importance of ferroptosis in the pathogenesis of multiple diseases, such as cardiomyopathy (38), several neurologic diseases (39), Parkinson's Disease (40) and cancers (41). Researches also showed that ferroptosis played an important role in endothelial cytotoxicity, and the mtROS-AMPK-ULK1 signaling pathway is probably involved in regulating the ferroptosis of endothelial cells. Furthermore, supplementation with ferrostatin-1(a potent inhibitor of ferroptosis,) remarkably reversed vascular injury (42).

Ferritin is a 24-subunit spherical shell protein composed of both light (FTL) and heavy chain (FTH1) subunits (43). Ferritin plays an important antioxidant role in cells by sequestering redox-active iron. Recent studies demonstrated that ferritin is a key ferroptosis regulator, which can affect the susceptibility to ferroptosis in vitro and in vivo (40,44,45). Both chains are essential for maintaining iron homeostasis and preventing iron overload (46,47). FTH1, involved in a variety of disease signaling pathways (40), is the functional subunit of the major iron storage protein ferritin, which possesses ferroxidase activity and efficiently reduces the toxicity of Fe2+ (48). Knockdown of FTH1 in the intestines of mice can lead to iron overabsorption and promote ferroptosis (49). Overexpression of FTH1 can suppress cell death induced by ferroptosis (41). In our study, the expression of FTL and FTH1 significantly decreased after treatment of DS, leading to the ferroptosis of IHUVECs. This finding suggests that such changes in Ferritin may be involved in the therapeutic effects of WJTLD.

In conclusion, the results from the present findings showed that the Chinese medicine Wenjingtongluo decoction has a significant effect on antiangiogenesis in IHUVECs. Moreover, the present TMT quantitative proteomics study identifies a repertoire of differentially regulated proteins on IHUVECs in response to treatment with drug-contained serum. These identified molecular targets of DS on HUVECs mediate a broad spectrum of antiangiogenic functions which encompass many pathways. Furthermore, major proteins from ferroportin were verified by PRM analysis. This work may provide proteomics clues for the continuation researches on WJTLD in antiangiogenesis, therefore highlighting the potential of WJTLD for therapeutic intervention against angiogenesis-related pathogenesis

Consent for publication
Not applicable.

Competing interests
All authors declare that they have no competing interests.

References

1. Lai SL, Wong PF, Lim TK, Lin Q, Mustafa MR. iTRAQ-based proteomic identification of proteins involved in anti-angiogenic effects of Panduratin A on HUVECs. Phytomedicine 2015 Jan 15; 22(1): 203-212. https://doi.org/10.1016/j.phymed.2014.11.016

2. Lei L, Ei Mourabit H, Housset C, Cadoret A, Lemoinne S. Role of Angiogenesis in the Pathogenesis of NAFLD. J Clin Med 2021 Mar 24; 10(7): 1338. https://doi.org/10.3390/jcm10071338

3. Baek A, Kim Y, Lee JW, Lee SC, Cho SR. Effect of Polydeoxyribonucleotide on Angiogenesis and Wound Healing in an *In Vitro* Model of Osteoarthritis. Cell Transplant 2018 Nov; 27(11): 1623-1633. https://doi.org/10.1177/0963689718804130

4. Folkman J. Angiogenesis inhibitors: a new class of drugs. Cancer Biol Ther 2003 Jul-Aug; 2(4 Suppl 1): S127-33.

5. Yetkin-Arik B, Kastelein AW, Klaassen I, Jansen CH, Latul YP, Vittori M, Biri A, Kahraman K, Griffioen AW, Amant F, Lok CA. Angiogenesis in gynecological cancers and the options for anti-angiogenesis therapy. Biochim Biophys Acta Rev Cancer 2020 Jan 1; 1875(1): 188446. https://doi.org/10.1016/j.bbcan.2020.188446

6. Mapp PI, Walsh DA. Mechanisms and targets of angiogenesis and nerve growth in osteoarthritis. Nat Rev Rheumatol 2012 May 29; 8(7): 390-398. https://doi.org/10.1038/nrrheum.2012.80

7. Walsh DA, McWilliams DF, Turley MJ, Dixon MR, Fransès RE, Mapp PI, Wilson D. Angiogenesis and nerve growth factor at the osteochondral junction in rheumatoid arthritis and osteoarthritis. Rheumatology (Oxford) 2010 Oct; 49(10): 1852-1861. https://doi.org/10.1093/rheumatology/keq188

8. Gordan JD, Kennedy EB, Abou-Alfa GK, Beg MS, Brower ST, Gade TP, Goff L, Gupta S, Guy J, Harris WP, Iyer R, Jaiyesimi I, Jhawer M, Karippot A, Kaseb AO, Kelley RK, Knox JJ, Kortmansky J, Leaf A, Remak WM, Shroff RT, Sohal DPS, Taddei TH, Venepalli NK, Wilson A, Zhu AX, Rose MG. Systemic Therapy for Advanced Hepatocellular Carcinoma: ASCO Guideline. J Clin Oncol 2020 Dec 20; 38(36): 4317-4345. https://doi.org/10.1200/JCO.20.02672

9. Nagai T, Sato M, Kobayashi M, Yokoyama M, Tani Y, Mochida J. Bevacizumab, an anti-vascular endothelial growth factor antibody, inhibits osteoarthritis. Arthritis Res Ther 2014 Sep 18; 16(5): 427. https://doi.org/10.1186/s13075-014-0427-y

10. Weixia J, Xiujuan H, Wenyan S, et al. Effects of Wenjing Tongluo method on gene expression of VEGF and its receptors in joint synovial tissues of CIA rats [J]. Beijing Traditional Chinese medicine 2014; 33(3): 211-214.

11. Weixia J, Zhu Y, Zhou HX, et al. Wenjing Tongluo method for the intervention of angiogenesis in rats with collagenous arthritis [J]. World Journal of integrated traditional Chinese and Western medicine 2013; (5): 502-506.

12. Xu WM, Qian JJ, Han L, et al. Effects of Wenjing Tongluo Decoction on cartilage morphological changes and expression of VEGF, MMP 13 and HIF-1 in mice with knee osteoarthritis. Chinese Medicine Information 2020; 37(6): 6-12.

13. Xu Q, Qian J, Xu W, Huang G, Ma Y, Guo Y, Han L, Wang L. effects of Wenjing Tongluo Decoction on VEGF/VEGFR2/ERK1/2 signaling pathway in a knee osteoarthritis model mouse. Zhongguo Shi Yan Fang Ji Xue Za Zhi 2021; 24: 28-34.

14. Liu T, Zhou J, Cui H, Li P, Luo J, Li T, He F, Wang Y, Tang T. iTRAQ-based quantitative proteomics reveals the neuroprotection of rhubarb in experimental intracerebral hemorrhage. J Ethnopharmacol 2019 Mar 25; 232: 244-254. https://doi.org/10.1016/j.jep.2018.11.032

15. Liu X, Guo DA. Application of proteomics in the mechanistic study of traditional Chinese medicine. Biochem Soc Trans 2011 Oct; 39(5): 1348-1352. https://doi.org/10.1042/BST0391348

16. Hughes CS, Spicer V, Krokhin OV, Morin GB. Investigating Acquisition Performance on the Orbitrap Fusion When Using Tandem MS/MS/MS Scanning with Isobaric Tags. J Proteome Res 2017 May 5; 16(5): 1839-1846. https://doi.org/10.1021/acs.jproteome.7b00091

17. O'Brien DP, Timms JF. Employing TMT quantification in a shotgun-MS platform. Methods Mol Biol 2014; 1156: 187-199. https://doi.org/10.1007/978-1-4939-0685-7_12

18. Zecha J, Satpathy S, Kanashova T, Avanessian SC, Kane MH, Clauser KR, Mertins P, Carr SA, Kuster B. TMT labeling for the masses: A robust and cost-efficient, in-solution labeling approach. Mol Cell Proteomics 2019 Jul; 18(7): 1468-1478. https://doi.org/10.1074/mcp.TIR119.001385

19. Overall CM. Can proteomics fill the gap between genomics and phenotypes? J Proteomics 2014 Apr 4; 100: 1-2. https://doi.org/10.1016/j.jprot.2014.02.025

20. DeCicco-Skinner KL, Henry GH, Cataisson C, Tabib T, Gwilliam JC, Watson NJ, Bullwinkle EM, Falkenburg L, O'Neill RC, Morin A, Wiest JS. Endothelial cell tube formation assay for the in vitro study of angiogenesis. J Vis Exp 2014 Sep 1; (91): e51312. https://doi.org/10.3791/51312

21. Zhang XH, Li CY, Lin QH, He ZH, Feng F, He MF. Pro-angiogenic activity of isoliquiritin on HUVECs in vitro and zebrafish in vivo through Raf/MEK signaling pathway. Life Sci 2019 Apr 15; 223: 128-136. https://doi.org/10.1016/j.lfs.2019.03.026

22. Qian JJ, Xu Q, Xu WM, Cai R, Huang GC. Expression of VEGF-A Signaling Pathway in Cartilage of ACLT-induced Osteoarthritis Mouse Model. J Orthop Surg Res 2021 Jun 14; 16(1): 379. https://doi.org/10.1186/s13018-021-02528-w

23. Ponting CP, Russell RR. The natural history of protein domains. Annu Rev Biophys Biomol Struct 2002; 31: 45-71. https://doi.org/10.1146/annurev.biophys.31.082901.134314

24. Wang ZD, Wei SQ, Wang QY. Targeting oncogenic KRAS in non-small cell lung cancer cells by phenformin inhibits growth and angiogenesis. Am J Cancer Res 2015 Oct 15; 5(11): 3339-3349.

25. Aird WC. The role of the endothelium in severe sepsis and multiple organ dysfunction syndrome. Blood 2003 May 15; 101(10): 3765-3777. https://doi.org/10.1182/blood-2002-06-1887

26. Li Y, Zhu H, Wei X, Li H, Yu Z, Zhang H, Liu W. LPS induces HUVEC angiogenesis in vitro through miR-146a-mediated

27. TGF-β1 inhibition. Am J Transl Res 2017 Feb 15;9(2):591-600.

27. Park HJ, Zhang Y, Georgescu SP, Johnson KL, Kong D, Galper JB. Human umbilical vein endothelial cells and human dermal microvascular endothelial cells offer new insights into the relationship between lipid metabolism and angiogenesis. Stem Cell Rev 2006; 2(2): 93-102. https://doi.org/10.1007/s12015-006-0015-x

28. Chang MW, Grillari J, Mayrhofer C, Fortschegger K, Allmaier G, Marzban G, Katinger H and Voglauer R: Comparison of early passage, senescent and hTERT immortalized endothelial cells. Exp Cell Res 2005 Sep 10; 309(1): 121-136. https://doi.org/10.1016/j.yexcr.2005.05.002

29. Böcker W, Yin Z, Drosse I, Haasters F, Rossmann O, Wierer M, Popov C, Locher M, Mutschler W, Docheva D, et al: Introducing a single-cell-derived human mesenchymal stem cell line expressing hTERT after lentiviral gene transfer. J Cell Mol Med 2008 Aug; 12(4): 1347-1359. https://doi.org/10.1111/j.1582-4934.2008.00299.x

30. Ozer HL, Banga SS, Dasgupta T, Houghton J, Hubbard K, Jha KK, Kim SH, Lenahan M, Pang Z, Pardinas JR, Patsalis PC. SV40-mediated immortalization of human fibroblasts. Exp Gerontol 1996 Jan-Apr; 31(1-2): 303-310. https://doi.org/10.1016/0531-5565(95)00024-0

31. Ouellette MM, McDaniel LD, Wright WE, Shay JW, Schultz RA. The establishment of telomerase immortalized cell lines representing human chromosome instability syndromes. Hum Mol Genet 2000 Feb 12; 9(3): 403-411. https://doi.org/10.1093/hmg/9.3.403

32. Srivastava RK, Unterman TG, Shankar S. FOXO transcription factors and VEGF neutralizing antibody enhance antiangiogenic effects of resveratrol. Mol Cell Biochem 2010 Apr; 337(1-2): 201-212. https://doi.org/10.1007/s11010-009-0300-5

33. Kim KH, Park GW, Jeong JE, Ji ES, An HJ, Kim JY, Yoo JS. Parallel reaction monitoring with multiplex immunoprecipitation of N-glycoproteins in human serum for detection of hepatocellular carcinoma. Anal Bioanal Chem 2019 May; 411(14): 3009-3019. https://doi.org/10.1007/s00216-019-01775-5

34. Malchow S, Loosse C, Sickmann A, Lorenz C. Quantification of cardiovascular disease biomarkers in human platelets by targeted mass spectrometry. Proteomes 2017 Nov 15; 5(4): 31. https://doi.org/10.3390/proteomes5040031

35. Aebersold R, Burlingame AL, Bradshaw RA. Western blots versus selected reaction monitoring assays: time to turn the tables? Mol Cell Proteomics 2013 Sep; 12(9): 2381-2382. https://doi.org/10.1074/mcp.E113.031658

36. Dixon SJ, Lemberg KM, Lamprecht MR, Skouta R, Zaitsev EM, Gleason CE, Patel DN, Bauer AJ, Cantley AM, Yang WS, Morrison B 3rd, Stockwell BR. Ferroptosis: an iron-dependent form of nonapoptotic cell death. Cell 2012 May 25; 149(5): 1060-1072. https://doi.org/10.1016/j.cell.2012.03.042

37. Stockwell BR, Friedmann Angeli JP, Bayir H, Bush AI, Conrad M, et al. Ferroptosis: A Regulated Cell Death Nexus Linking Metabolism, Redox Biology, and Disease. Cell 2017 Oct 5; 171(2): 273-285. https://doi.org/10.1016/j.cell.2017.09.021

38. Fang X, Wang H, Han D, Xie E, Yang X, Wei J, Gu S, Gao F, Zhu N, Yin X, Cheng Q. Ferroptosis as a target for protection against cardiomyopathy. Proc Natl Acad Sci U S A. 2019 Feb 12; 116(7): 2672-2680. https://doi.org/10.1073/pnas.1821022116

39. Weiland A, Wang Y, Wu W, Lan X, Han X, Li Q, Wang J. Ferroptosis and its role in diverse brain diseases. Mol Neurobiol 2019 Jul; 56(7): 4880-4893. https://doi.org/10.1007/s12035-018-1403-3

40. Tian Y, Lu J, Hao X, Li H, Zhang G, Liu X, Li X, Zhao C, Kuang W, Chen D, Zhu M. FTH1 inhibits ferroptosis through ferritinophagy in the 6-OHDA model of Parkinson's disease. Neurothe-

rapeutics 2020 Oct; 17(4): 1796-1812. https://doi.org/10.1007/s13311-020-00929-z

41. Kong N, Chen X, Feng J, Duan T, Liu S, Sun X, Chen P, Pan T, Yan L, Jin T, Xiang Y, Gao Q, Wen C, Ma W, Liu W, Zhang M, Yang Z, Wang W, Zhang R, Chen B, Xie T, Sui X, Tao W. Baicalin induces ferroptosis in bladder cancer cells by downregulating FTH1. Acta Pharm Sin B 2021 Dec; 11(12): 4045-4054. https://doi.org/10.1016/j.apsb.2021.03.036

42. Qin X, Zhang J, Wang B, Xu G, Yang X, Zou Z, Yu C. Ferritinophagy is involved in the zinc oxide nanoparticles-induced ferroptosis of vascular endothelial cells. Autophagy 2021 Dec; 17(12): 4266-4285. https://doi.org/10.1080/15548627.2021.1911016

43. Muhoberac BB, Vidal R. Iron, Ferritin, Hereditary Ferritinopathy, and Neurodegeneration. Front Neurosci 2019 Dec 11; 13: 1195. https://doi.org/10.3389/fnins.2019.01195

44. Masaldan S, Bush AI, Devos D, Rolland AS, Moreau C. Striking while the iron is hot: Iron metabolism and ferroptosis in neurodegeneration. Free Radic Biol Med 2019 Mar; 133: 221-233. https://doi.org/10.1016/j.freeradbiomed.2018.09.033

45. Fang Y, Chen X, Tan Q, Zhou H, Xu J, Gu Q. Inhibiting Ferroptosis through Disrupting the NCOA4-FTH1 Interaction: A New Mechanism of Action. ACS Cent Sci 2021 Jun 23; 7(6): 980-989. https://doi.org/10.1021/acscentsci.0c01592

46. Sammarco MC, Ditch S, Banerjee A, Grabczyk E. Ferritin L and H subunits are differentially regulated on a post-transcriptional level. J Biol Chem 2008 Feb 22; 283(8): 4578-4587. https://doi.org/10.1074/jbc.M703456200

47. Friedman A, Arosio P, Finazzi D, Koziorowski D, Galazka Friedman J: Ferritin as an important player in neurodegeneration. Parkinsonism Relat Disord 2011 Jul;17(6):423-430. https://doi.org/10.1016/j.parkreldis.2011.03.016

48. Salatino A, Aversa I, Battaglia AM, Sacco A, Di Vito A, Santamaria G, Chirillo R, Veltri P, Tradigo G, Di Cello A, Venturella R, Biamonte F, Costanzo F. H-Ferritin affects cisplatin-induced cytotoxicity in ovarian cancer cells through the modulation of ROS. Oxid Med Cell Longev 2019 Oct 31; 2019: 3461251. https://doi.org/10.1155/2019/3461251

49. Sun X, Ou Z, Chen R, Niu X, Chen D, Kang R, Tang D: Activation of the p62-Keap1-NRF2 pathway protects against ferroptosis in hepatocellular carcinoma cells. Hepatology 2016 Jan; 63(1): 173-184. https://doi.org/10.1002/hep.28251